Tellus (2004), 56A, 167–175
Printed in UK. All rights reserved

TELLUS

Accuracy of the modelled wind and wave fields in enclosed seas

By LUIGI CAVALERI* and LUCIANA BERTOTTI, *ISMAR, S. Polo 1364, 30125 Venice, Italy*

(Manuscript received 30 September 2002; in final form 10 September 2003)

ABSTRACT

The meteorological model of the European Centre for Medium-Range Weather Forecasts, run with different resolutions, has been used to explore, with a number of numerical experiments, the underestimate of wind speeds and wave heights found in enclosed basins. Comparisons have been made between the results from the different runs, and also against satellite and buoy data.

It is found that the error depends on fetch, i.e. on the distance from the closest land from which the wind is blowing. Large errors are found at short fetches (order of 100 km), gradually decreasing with the distance from the coast. The error is larger and more persistent for waves. Increasing the resolution leads to an improvement of the results. However, the bias does not disappear at the highest resolution we have used (about 25 km).

Experiments with the single-point version of the meteorological model do not suggest that a slow development of the marine boundary layer is the main reason for the underestimate of the wind speeds. With respect to the mean orography, the use of envelope orography leads to a substantial increase of the marine wind speeds in the area affected by land.

1. Introduction

The present quality of the modelled surface wind fields over the oceans is generally good. Comparisons with independent data suggest, e.g. for the European Centre for Medium-Range Weather Forecasts (ECMWF, Reading, UK) an average bias of 5 cm s^{-1}, and a scatter index SI = 0.18 (see Janssen et al., 2000; Abdalla et al. 2002). The values are slightly larger in the local winter and smaller in summer. The peak values in areas with strong gradients are still often underestimated, but on the whole the situation is satisfactory.

The conditions are different in enclosed basins, and more generally whenever the surface wind fields are affected by the presence of land. In these areas the marine modelled surface wind speeds are almost always underestimated, with the bias depending on the proximity of land (see, e.g., Cavaleri and Bertotti, 1997). This negative effect is felt for relatively large distances, so that the problem also appears in large basins, such as the Mediterranean Sea.

As expected, the modelled wave fields, obtained using the wind fields as input, reflect the same characteristics. They are good on the oceans, where the bias of the significant wave height, measured on a global scale, is 5 cm, with SI = 0.12 (Abdalla et al. 2002). The quality drops drastically when we move to the enclosed basins. An extensive comparison against the recorded data from a number of directional buoys distributed along the Italian coastline shows an average underestimate of almost 30%, with local maxima beyond 40%.

A lack of resolution is considered to be the main reason for the underestimate of the wind speeds in coastal areas (see, e.g., Pielke, 2002). The accuracy with which the geometry of the coastline is described in the model is limited by its resolution. Therefore it is natural to expect a poorer quality of the surface wind fields in the proximity of land, even more so if the coast is characterised by a pronounced orography. Within the effort by the major meteo-oceanographic centres to increase their computer power and the resolution of their meteorological model, it is of interest to explore how much this will lead to an improvement in the final results, in particular of the surface wind speeds and associated wave heights. With this in mind, we have carried out a series of experiments with different resolutions, and compared the results among themselves and against the available measurements. In this paper we describe the tests and their results.

The structure of the paper is as follows. In Section 2 we present the organisation of the experiments and the periods considered. In Section 3 we intercompare the results obtained with the different resolutions, and also provide an evaluation of their absolute performance. In Section 4 we focus on the orography of the area bordering the basin of interest, and on its effects on the marine wind and wave fields. The influence of land is further

*Corresponding author.
e-mail: luigi.cavaleri@ismar.cnr.it

highlighted in Section 5, where we study how the model results improve on moving far from the land the wind is blowing from. In Section 6 we explore possible reasons for the underestimate found in the enclosed basins. The conclusions are summarised in the final section.

2. The structure of the tests

The Mediterranean Sea has been chosen as a test area. It is a very active basin, enclosed between Africa and Europe, and hence between two contrasting climates. Its dimensions, more than 4000 km in longitude and 1600 km in latitude, are large enough to allow the development of severe storms. At the same time, its complicated geometry and the orography that characterises most of its coastline provides examples of sub-basins at different scales.

The climate is often calm, with intermittent stormy periods, especially in winter. Therefore, for our analysis, rather than a prolonged continuous period, we have preferred to focus on a series of separate events. This has also allowed a choice compatible with the various kinds of storms that typify the basin. Table 1 lists the events chosen for the analysis.

Each event has been modelled with different resolutions R of the meteorological model. For this we have made use of the operational model at ECMWF. This is a spectral model (Simmons, 1991), the resolution of which is typified (e.g. T511) by the truncation level of the two-dimensional Fourier series used to describe the horizontal fields. T511 is the resolution of the model presently operational at ECMWF. For our tests we have considered both higher and lower resolutions. This has allowed us to obtain a better perspective on how the quality of the results varies with R. Table 2 shows the values of R we have used, together with their corresponding spatial resolutions.

For each R value, each storm has been modelled with a sequence of short-term (72-h) forecast experiments, each starting typically two days after the previous one. From their output, a continuous sequence of surface wind fields at 6-h intervals has been obtained, using for each experiment intervals from +24 to +66 h (see Fig. 1). The underlying principle was to limit the extent of the forecast to avoid large divergences with respect to the analysis, allowing enough time for the model to develop the characteristics of its resolution. An extension of this principle was adopted at the beginning and at the end of the storm to consider the whole period.

Table 1. Periods considered for the experiments

1	9–12 Jan 1987
2	31 Dec 1992–12 Jan 1993
3	4–12 Feb 1994
4	8–17 Jan 1995
5	18–21 Mar 1995
6	26 Mar–1 Apr 1995
7	27 Dec 2000–1 Jan 2001

Table 2. Spectral resolution for different truncation levels T

T	106	213	319	511	639	799
Resolution (km)	190	95	63	39	31	25

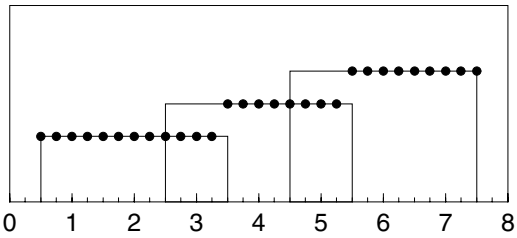

Fig 1. Sequence of partially overlapping forecast experiments. The dots indicate the fields chosen for the analysis. Units are days.

All the experiments were performed in coupled mode (Janssen, 1989, 1991), i.e. with the wave model running in parallel to the meteorological one, with a continuous exchange of information on the roughness of the sea surface. However, experiments on a global scale, where the resolution of the wave model is 0.5°, cannot properly describe the wave fields in the Mediterranean Sea (Cavaleri et al. 1991). Therefore the time series of wind fields previously obtained has been used to drive a 0.25° resolution wave model. As in the global coupled experiments, the wave model was WAM (Komen et al. 1994), a state of the art third-generation model, where the evolution of the wave field is modelled on a purely physical basis, without any parametrisation or a priori assumption on the shape of the spectrum. These second runs were performed in uncoupled mode, i.e. the information was flowing only from wind to waves. This had little relevance, because the winds had already been obtained in coupled mode.

The set of storms listed in Table 1 provided 46 days (184 fields) of wind and wave simulation. Repeated for different Rs listed in Table 2, this provided a good data set suitable for analysis.

3. Comparison of results with different resolutions

We begin our analysis with an intercomparison of the results obtained with different resolutions. To obtain a better perception of how the quality changes with R, we compare the resolutions in sequential order, i.e. T106 versus T213, T213 versus T319, and so on (see Table 2). One example is given in Fig. 2, T106 versus T213, with the scatter diagrams of the corresponding wind speed U_{10} and wave heights H_s for all the storms considered. The overall results, as the slope of the best-fitting lines, are given in Table 3. We see the progressive increase of U_{10}, and hence H_s, when the resolution is increased.

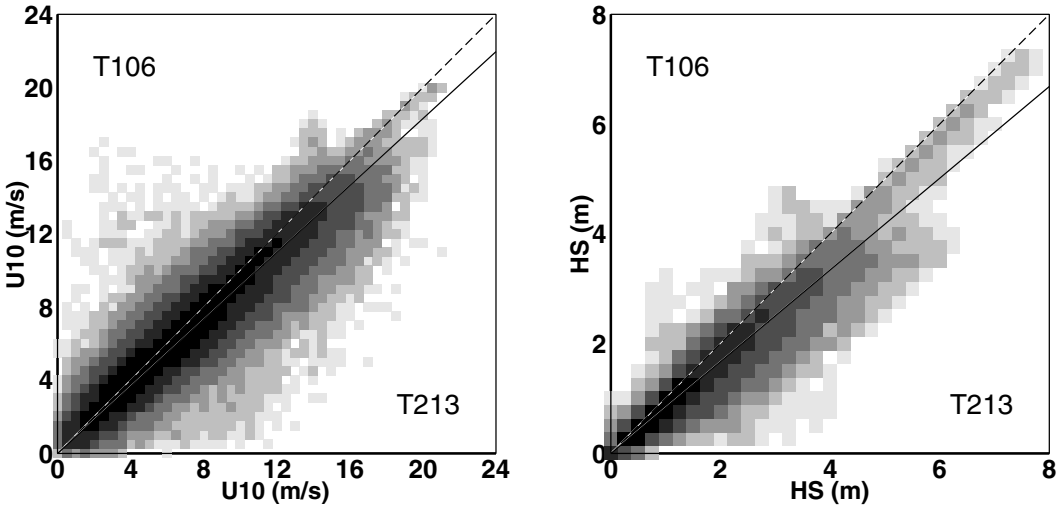

Fig 2. Comparison between wind speeds (left-hand panel) and wave heights (right-hand panel) from experiments with different resolutions. Darker pixels include larger amounts of data.

Table 3. Best-fitting slope, for wind speed and wave height, between corresponding results from different spectral resolutions

T/*T*	106/213	213/319	319/511	511/639	639/799
Wind	0.910	0.984	0.974	0.986	0.995
Waves	0.848	0.959	0.952	0.985	0.988

The general trend is better seen in Fig. 3, where the above results are plotted, normalised with respect to T106. For comparison we also show the results for the open oceans. Note that, due to the different climates that characterise the oceans and the Mediterranean Sea, they have different T106 normalisation factors.

In the oceans both the wind and wave values have a tendency to give an asymptotic behaviour. This suggests that with the present ECMWF model T511, and even more so with higher resolutions, the results are very close to the correct values, as indeed it is the case, as proved by the statistics reported in the introduction.

The situation in the Mediterranean Sea is quite different. Every increase of resolution leads to a substantial increase of both U_{10} and H_s, and it is only with the highest resolutions that we find indications of an asymptotic behaviour. This strongly suggests that, even with T799, we are below the correct values.

This is better quantified by comparing the results against measured data. The quality of the wind speeds has been evaluated with respect to the data obtained from the ERS1-2 scatterometer. Having worked with forecast experiments, without any data assimilation, the comparison was objective. In general, the data are not available at the same time and location (grid points) of the model data. Therefore the latter ones have been linearly interpolated in space and time to derive the model value corresponding to each remote measure. A scatter diagram of the co-located pairs of values, and the corresponding best-fitting slope provides a fair estimate of the performance of the model. The results are again shown in Fig. 3 (left-hand panel), where the horizontal dotted lines represent, with respect to T106, the measured values. So we see that at the highest resolution the wind speeds in the Mediterranean Sea are indeed approaching the measured value, with the bias being reduced to less than 2%. Of course this is reflected in the quality of the wave results (right-hand panel). For H_s the comparison has been done against the Topex altimeter measured wave heights. Here too the increase of resolution led to a progressive approach to the average measured value. However, given the sensitivity of the wave field to variations of the input wind field, the differences among the resolutions are larger than for wind. For the same reason, for each R the percentage H_s bias is larger than for U_{10}. At T799 the H_s values are too low by 6%.

4. Influence of the orography

A higher resolution implies a better description of the orography, which has obvious consequences on the modelled wind fields, particularly when the wind blows from land to sea. Table 4 reports the maximum height and the average sub-grid variability σ of the orography for an area (longitude 6–14° E, latitude 44–48° N) including the Alps, according to the different resolutions. σ is evaluated with respect to a high-resolution (5-km) reference orography. The higher the resolution is the smaller the σ value, because the mean orography succeeds in following the reference better. It is clear that the more detailed description available in T799 implies more detailed and more spatially varying wind fields. Figure 4 (left-hand panel) shows a case of the mistral in the Gulf of Lions, in the northwest part of the Mediterranean Sea. The jet blows down from the Carcassone pass, between the

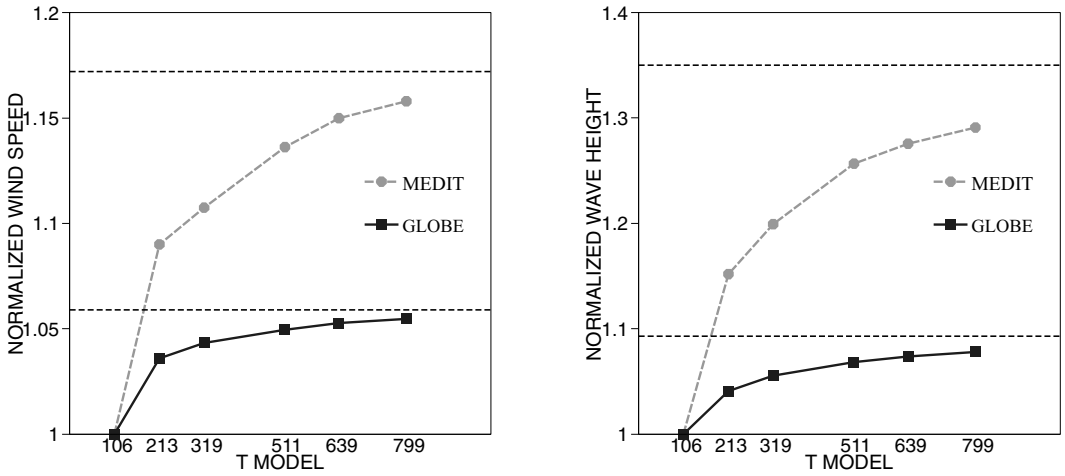

Fig 3. Nondimensional increase of wind speed and wave height with increased resolution. T106 is taken as a reference. The values are given for the global oceans and for the Mediterranean Sea. The horizontal dotted lines show the corresponding sea truths as derived from the ERS1-2 scatterometer.

Table 4. Maximum height and mean root mean square error σ (m) of the orography described with different spectral resolutions T. The area considered is from 6 to 14° E and from 44 to 48° N. The reference orography for the evaluation of σ has 5-km resolution

T	106	213	319	511	639	799
Max h	1346	1901	2087	2262	2388	2445
Mean σ	439	327	327	257	242	224

Pyrenees and the Massif Central. Its structure is strongly controlled by the local orography. We consider a transverse section of the jet, A–B, and the related distribution of the wind speed U_{10} for every resolution R (right-hand panel), plus the evidence from the scatterometer data. It is clear that the lower resolutions tend to smooth the field. The more detailed description of, for example, T799, leads to a narrower jet, and consequently to higher wind speeds (maximum speed 19.6 m s^{-1} against 16.4 m s^{-1} for T213). However, apart from the error in the basic distribution, even T799 (spatial resolution 25 km) does not succeed in reproducing the detailed variability visible in the scatterometer profile.

That a better description of the orography leads to a better description of the nearby wind fields is hardly surprising. Channelling, downslope winds, valley jets, shadowing are all expected features, only partially reflected in the modelled winds, the degree of accuracy depending on the resolution. Olafsson and Bougeault (1996), Laing and Brenstrum (1996), Doyle and Shapiro (1999), Zecchetto and Cappa (2001), among others, give good examples of this. For our present interests the further relevant point is that a higher R value also leads to higher average wind speeds. This has been clearly shown in the previous section.

Both of these points have implications for the wave heights. Obviously higher U_{10} values imply higher H_s. However, spatial variability also has a role. The waves are an integrated effect, in space and time, of the generating wind fields. Therefore their distribution does represent, in a partially smoothed way, the spatial distribution of the wind. Besides, due to the nonlinear processes that characterise the wind wave generation (Abdalla and Cavaleri, 2002), any spatial and temporal variability of U_{10} leads on average to an increase of H_s.

All of this suggests that the fit between the model and, for example, the scatterometer data is not uniform throughout the Mediterranean Sea. Rather, we expect it to be characterised by a marked spatial variability. The data set derived from our experiments is not fully suitable for such an analysis. With only 184 values per grid point (see Section 2) and only a fraction of them corresponding to a scatterometer passage, it is not possible to derive reliable statistics. Therefore we have considered the analysis results of ECMWF from 1992 to 1998, available at 6-h intervals (00, 06, 12, 18 UTC). In this period the resolution was T213. The surface winds have been extracted with 0.5° resolution, similar to what was done in our experiments. As a reference we have used the wind speed and wave height data from the Topex altimeter. Following the same interpolation procedure described in the previous section, we have obtained a series of co-located satellite and model data. Each pair has been assigned to the closest grid point. Six years of data have provided enough data for reliable statistics. Figure 5 shows an example of the best fit. There is considerable scatter, related to improperly modelled variability of the atmosphere (Abdalla and Cavaleri, 2002), but also to the varying capability of the model to reproduce the different meteorological situations. This has suggested a smoothing of the spatial distribution of the best-fitting slopes.

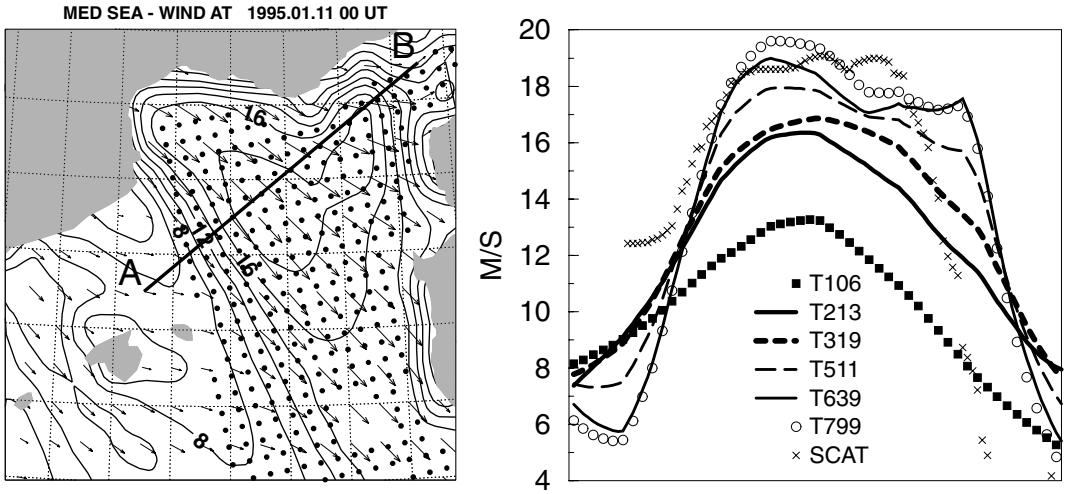

Fig 4. A case of mistral (left-hand panel) in the Western Mediterranean Sea. The isotachs are drawn at 2 m s^{-1} interval. The arrows show the direction and intensity of the surface wind field, according to the T639 resolution. The dots show the official locations where scatterometer measurements are available. The wind speed profile along the A–B section is given in the right-hand panel, for the scatterometer and for the different resolutions of the meteorological model.

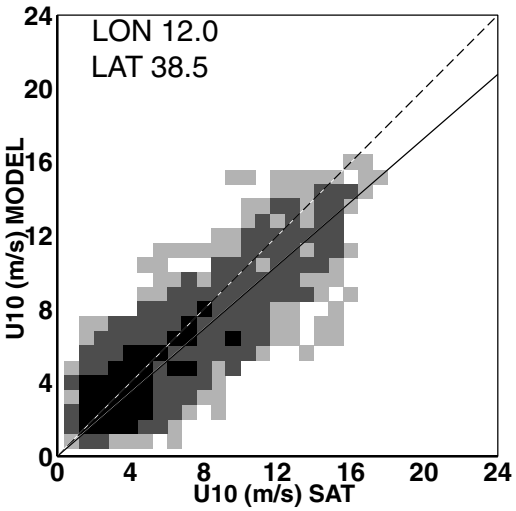

Fig 5. Comparison between the modelled wind speed values and the corresponding Topex altimeter data for one location in the Mediterranean Sea. Six years of ECMWF analysis data (1992–1998) have been considered. Darker pixels include larger amounts of data.

Although this may hide some very local details, it provides a more reliable general pattern.

The resulting distribution for wind speed is shown in Fig. 6. The main characteristic is the strong underestimate, up to 50%, in the northern part of the basin, gradually attenuating when we move towards the southern coasts. This reflects two facts: the more complicated orography along the northern border of the Mediterranean Sea, and the dominant directions (between west and northeast) where the storms come from. Superimposed on this trend, there is spatial variability, connected to the most relevant orographic features, e.g. the Alps, and to the dimensions of the sub-basins. Obvious examples are the Ligurian and the Adriatic seas, respectively to the west and east of Italy, and the Aegean Sea.

The corresponding distribution for the wave heights (not shown) has similar, but enhanced, features, due to the relationship between H_s and U_{10}. In the three considered sub-basins the underestimate of H_s goes up to 50%, with much lower values, between 10 and 20%, along the African coastline.

5. The fetch dependence

The distribution of the wind bias in Fig. 6, together with the main direction the storms come from, strongly suggests that the model wind bias decreases with fetch. As mentioned in the previous section, the same is true for waves. To obtain a more objective verification of this hypothesis, we have analysed the percentage error b of the model wave heights with respect to the data collected by eight measuring buoys distributed along the Italian coastline (Franco and Contini, 1997). b has been plotted as a function of fetch f, defined as the length of sea run by the waves during their generation by wind. A straightforward approach could be to consider for each measurement the direction the waves were coming from, and to find from pure geography, in practice from the land–sea mask, the distance of the closest land in this direction. However, this could be misleading for several reasons: (1) the wind could have been blowing along only a part of this distance; (2) the generation is not always along straight lines; (3) the back-tracing ray could end on (or just miss) an island or a peninsula; and (4) the generation is not strictly along a mean line, but distributed on an angular sector. Therefore a more complete approach has been followed.

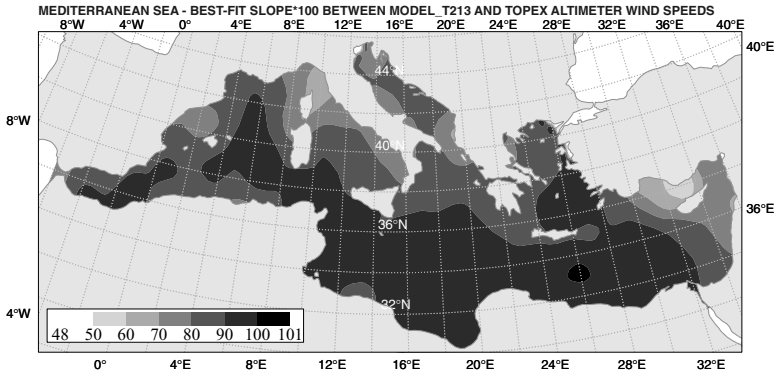

Fig 6. Distribution of the best-fitting slopes (see Fig. 5) in the Mediterranean Sea.

The fetch has been evaluated along seven different directions, distributed at 5° intervals around the mean incoming wave direction θ_o. For the final estimate their respective fetch lengths have been weighted with the squared cosine of the angle $\Delta\theta$ with respect to θ_o. Along each direction the fetch has been evaluated by backtracing the wave field in space and time, always moving with the local group speed (with which the wave energy propagates), and remaining at an angle $\Delta\theta$ with respect to the local wind direction. For each direction the procedure was stopped when any of the following conditions was met: reaching land, wind speed below 5 m s^{-1} or a mean wave period lower than 3 s. The information on the wind and wave fields was derived from the models. To minimise the consequences of model resolution on the description of the coastline or the effect of local winds, not properly represented in the global meteorological model, only cases with a fetch larger than 100 km and a wave height larger than 1 m have been used in the analysis.

The overall result is shown in Fig. 7. There is a large scatter, associated with the variability of the error and with the approximations involved in the evaluation of the fetch. However, the overall conclusion, summarised by the best-fitting line, is fairly clear: b depends drastically on f, decreasing from an average of 28% at short fetches to a few per cent for the longest distances (order of 1000 km).

It is fair to point out that the modelled H_s are the product of two models working in series. The coupling between the meteorological and the wave models (see Section 2) does not exclude the substantial dependence of the latter on the former. In principle the error could be in the wave model. However, it is by now amply accepted (see, e.g., Komen et al. 1994; Janssen, 1998) that the error of a wave model is smaller than the error of the driving wind fields. Therefore these are most likely to be the main source of the errors seen in Fig. 7.

We can verify the consistency of the wind and wave underestimates using the simple relationship $H_s \propto (U_{10})^{\beta}$ (see Komen et al. 1994), where β varies between 1 for very short fetches and 2 for fully developed seas. In the intermediate conditions of the Mediterranean Sea, as a first-order approximation we can assume $\beta = 1.5$. From this we derive $\Delta H_s = 1.5 \times \Delta U_{10}$, where Δ represents the percentage error. This suggests a wind speed bias of about 20% at short fetches, decreasing with the distance from the coast. This result is consistent with the independent validation against the satellite data described in the previous section (see Fig. 6).

It is of interest to see how the fetch dependence varies with the resolution of the meteorological model. Using the results of our experiments for this would have produced a very limited number of data points for each resolution, which would not have

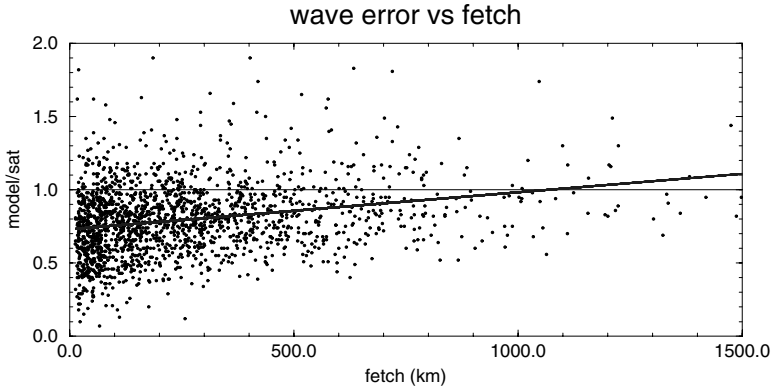

Fig 7. Distribution and best-fitting line of the nondimensional modelled wave height errors as a function of fetch (km).

Table 5. Percentage errors, for wind speed and wave height, at short fetches, for different spectral resolutions *T*

T	106	213	319	511	639	799
Wind	25	18	15	11	8	6
Waves	35	28	24	17	12	9

been sufficient for reliable statistics. Therefore we have extended the method by considering as reference measurements all the data, wind speeds and wave heights available from satellites. For each remote datum we have considered the corresponding model value, as described in Section 3, and evaluated the corresponding fetch (as with the buoys). The results are given in Table 5 as percentage errors at short fetches (100 km).

The underestimates for wind and waves are mutually consistent, further confirming the results. There is an expected improvement (higher values, i.e. lower underestimates) with the resolution. Note that the figures in Table 5 are larger than what was derived from Fig. 3. While the errors discussed in Section 3 represent an average of the whole field, in Table 5 we have reported only the errors at short fetches, which are the largest ones. As we have seen in Fig. 7, the errors rapidly decrease with fetch, but with different rates. On the average the wind error reaches very low values after 500–600 km, while for the waves this happens after 800–1000 km. As already mentioned, this depends on the memory the waves have of the early stages of generation.

Lower biases for longer fetches also imply lower differences between different resolutions. This can be verified for specific storms. An example is given in Fig. 8. The Adriatic Sea, between the Italian peninsula and the Balkan countries, has two dominant storm patterns. The sirocco (left-hand panel) blows northwards along its main axis (the maximum fetch is 700 km). It is channelled between the Apennines and the Dinaric Alps, but no mountain ridge is present in the direction it comes from. The bora (right-hand panel), a cold and gusty wind, blows from the northeast across the basin. The maximum fetch is 200 km. In the two panels we have plotted as isolines the percentage differences of wind speed between the T639 and T319 simulations. The vectors show the actual wind fields. The isolines are traced at 10% interval. It is evident that for the bora the differences are much larger. A detailed analysis of the difference field reveals for the bora values up to 70%. For the sirocco some large differences are present only in the lower and upper right-hand parts of the basin, where the fetch is short. Averaged over the whole basin, the differences are 1% for the sirocco (there are positive and negative difference values) and 18% for the bora.

6. Possible reasons for the underestimate at short fetches

In this section we further discuss possible reasons for the underestimate of model wind speeds at short fetches. Granted the influence of the resolution on the description of the geometry of the coast, this does not justify the substantial underestimate of wind speeds we also find at larger distances from the coast, up to several hundred kilometres.

When the air flows from land to sea, the reduced surface drag leads to the development of a new boundary layer, the thickness of which increases progressively with fetch, parallel to the increase of wind speed (see, e.g., Stull, 1988). It was suggested (by Anthomy Hollingsworth) that the underestimate could be connected to a slow development of the modelled boundary layer. We

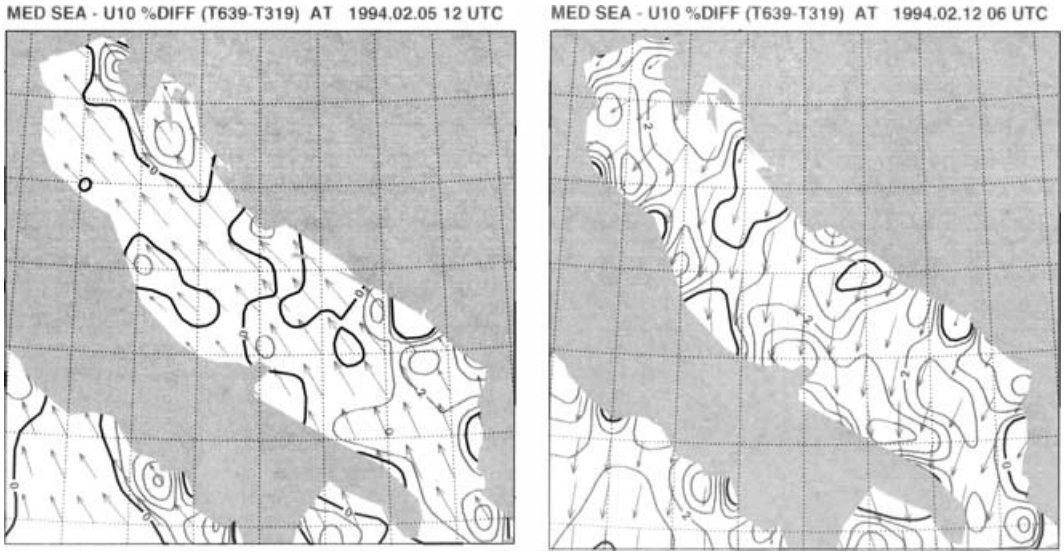

Fig 8. Cases of sirocco (left-hand panel) and bora (right-hand panel) in the Adriatic Sea. The arrows show the wind fields. The isolines, at 10% interval, show the percentage differences between the T639 and T319 simulations.

have explored this possibility by making use of the single-point (one-column) version of the ECMWF meteorological model. The model integrates a set of four prognostic equations (u, v, T, q, respectively the zonal and meridional components of wind speed, temperature and specific humidity) for a column of the atmosphere. In the soil there are evolution equations for the temperature and wetness of the different soil layers plus an evolution equation for the skin temperature and the skin water content. The one-column model can be used with prescribed forcing: the zonal and meridional components of the geostrophic wind, the vertical velocity and the horizontal advection of the atmospheric variables. The surface pressure is kept constant. The vertical advection is computed as part of the one-column integration using a semi-Lagrangian scheme. The height of the three lowest model levels is roughly 30, 150 and 300 m. For a more detailed description of the model see Teixeira (1997).

The model can be run for different latitudes and for different seasons, in practice varying the intensity and time of the solar radiation. Consistent with our area of interest, we chose 41°N and winter months. The model was initialised with 2 days of simulation on land (surface roughness 0.48537 m) to reach a stable daily cycle, after which we shifted to sea conditions (roughness 0.1×10^{-3} m). The details of the experiments are given in Cavaleri and Teixeira (2002). For our present purposes the relevant result is that there was no indication of a substantial delay in the development of the marine boundary layer, at least large enough to explain the fetch behaviour we have described above.

The second reason we considered was the description of the orography. Up until 1995 in the ECMWF meteorological model the so-called envelope orography (EO) was used. In EO the modelled height of the mountains equals the mean orography (MO) in each area, augmented by the quantity $\alpha\,\sigma$, where σ is the root mean square variability of the sub-grid orography and α is a coefficient between 0.5 and 2 (Wallace et al. 1983; Tibaldi, 1986). In April 1995 the envelope orography was replaced by the mean value, because this turned out to be beneficial for the medium range forecast (Miller et al. 1995; Lott and Miller, 1997).

Our attention was stimulated by a specific aspect of the results from our experiments. It was customary to compare the results of each run with the original analysis. Most of our experiments (2–6, see Table 1) refer to a period for which T213 was used. It was a surprise to find that the analysis wind speeds in the Mediterranean Sea were in general higher than those from our experiments, whatever the resolution. This was particularly true in the areas affected by an offshore blowing wind. It turned out not to be the case with the most recent storm we analysed (no 7 of the list). All our experiments have been performed with the present default version of the model, i.e. with MO. Therefore the possibility was considered that the change from EO to MO had a direct influence on the coastal wind fields. This prompted a new series of experiments, where the event of January 1995 was simulated using the EO. The results were instructive. For all the resolutions the modelled wind and wave fields in the Mediterranean Sea were enhanced. In particular, in the Gulf of Lions, affected by the mistral, the wind peak value for T639 reached 20.7 m s^{-1}, compared with 19.0 m s^{-1} with MO and 19.8 m s^{-1} for the T213 analysis. The corresponding H_s values are 6.4 m (EO), 5.5 m (MO) and 5.6 m (analysis).

Passing from the EO to the MO, and hence to a lower height for the orographic obstacles, the decreased drag on the atmospheric flow was compensated by the introduction of a bluff body drag (Miller et al. 1995; Lott and Miller, 1997) that explicitly represents the blocking of the low-level flow and the associated form drag due to the flow separation caused by the sub-grid scale orography. Therefore it is logical not to consider it when using the EO. In this respect we point out that the experiments were repeated with and without the bluff body drag, but the results in the area of interest hardly showed any difference.

The suggestion we derive is that the mean orography, beneficial for the general forecast, leads to lower surface wind speeds with respect to the envelope orography. This appears in the marine areas on the lee of and affected by land. The differences are not sufficient to fill the gap between the modelled and the measured data, but they are certainly significant for the present errors.

7. Conclusions

The modelled marine surface wind speeds are underestimated in the enclosed basins, and, more generally, in the areas where the wind is blowing from land. We have explored the situation analysing a number of storms with a series of numerical experiments. We have used the meteorological model of ECMWF, run with different resolutions. Clear indications on the performance of the model have been obtained both intercomparing the results and using as reference the available measured data (satellite and buoys).

The overall findings can be summarised in the following points.

(1) The bias (practically always negative) of the modelled wind speeds U_{10} depends on the resolution of the model. Increasing the resolution leads not only to a better description of the details of the field, but also to an increase of the average U_{10}.

(2) For both wind and waves we have defined for each model datum a fetch length, as the length of the sea path, followed either by air or waves, to reach that location. Measured with respect to satellite data, the wind bias for the T319 version of the meteorological model (spatial resolution ∼63 km) varies from 15% at short fetches (about 100 km) to less than 3% at distances larger than 600 km. For the highest resolution we have used, T799, corresponding to about 25 km, the bias decreases respectively to 6% and a value very close to zero.

(3) The wave results follow accordingly. In general the percentage bias of the significant wave height H_s is larger than for

the wind speed, due to the nonlinear processes present in wave generation. Because of the longer memory of waves, the bias tend to persist for longer distances.

(4) The results mentioned in point (2) have been confirmed by a more extensive comparison done using the operational results of the ECMWF meteorological model from 1992 to 1998, when T213 was used (resolution of ∼95 km). The larger data set has allowed a more defined geographical distribution of the bias. The larger negative values, between 15 and 50%, are found close to the northern coasts of the Mediterranean Sea. They tend to decrease southwards. The overall pattern is associated with the geographical distribution of the orography, and with the dominant directions followed by the storms. The largest values for bias are found in the smaller basins surrounded by a complicated orography.

(5) A similar result has been obtained for the model wave heights, both compared with altimeter and buoy measurements. At short fetches the average underestimate is 28%. The largest values are found close to the northern coasts of the basin, with values up to 50% in the more enclosed seas, such as the Ligurian and the Northern Adriatic Sea. The bias decreases substantially moving southwards, where in the open waters in front of the African coast the value decreases to an average of 15%.

(6) Within the accuracy of the fetch dependence associated to the limited data set from our experiments, the results from the extensive comparison in points (4) and (5) are consistent with those mentioned in (2) and (3).

We have searched for possible reasons for the wind bias and its fetch dependence (the wave bias is just a consequence). In particular,

(7) using the single-point version of the ECMWF meteorological model, we have not found evidence that the bias is connected to a slow development of the marine boundary layer;

(8) in the ECMWF meteorological model the orography is represented as mean orography. We have found that the use of the envelope orography leads to a substantial increase of the surface wind speeds in the areas on the lee of and affected by land. The waves follow accordingly, with an increase of their peak value just off the coast close to 20% in the considered case.

8. Acknowledgements

The tests and the analyses described have been done mostly at the European Centre for Medium-Range Weather Forecasts, Reading, UK. There we have interacted with many people, in particular with Peter Janssen for the experiment with the envelope orography, Martin Miller, Anton Beljaars and Jean Bidlot. Joao Teixeira provided the one-column version of the meteorological model, the use of which was suggested by Anthony Hollingsworth. Finally, the user support group has been an essential help in using the local computer system. This research has been partially supported by the WEAO Euclid Project WWMEDATLAS.

References

Abdalla, S. and Cavaleri, L., 2002. Effect of wind variability and variable air density on wave modelling. *J. Geophys. Res.* **107**, No. C7, 17–1/17–17

Abdalla, S., Janssen, P. A. E. M. and Bidlot, J.-R. 2002. The use of satellite observations and enhanced physics to improve wind–wave predictions at ECMWF. *28th Int. Conf. on Coastal Eng.*, Cardiff, UK, 7–12 July 2002.

Cavaleri, L. and Bertotti, L. 1997. In search of the correct wind and wave fields in a minor basin. *Mon. Wea. Rev.*, **125**, 8, 1964–1975.

Cavaleri, L. and Teixeira, J. 2002. Oscillations in an offshore blowing wind. *Nuovo Cimento* **25**, 2, 175–183.

Cavaleri, L., Bertotti, L. and Lionello, P. 1991. Wind wave cast in the Mediterranean Sea. *J. Geophys. Res.* **96**, C6, 10 739–10 764.

Doyle, J. D. and Shapiro, M. A. 1999. Flow response to large-scale topography: the Greenland tip jet. *Tellus* **51A**, 728–748.

Franco, L. and Contini, P. 1997. Wave measurements and climatology of the Italian seas. *PIANC Bull.*, **94**, 536–544.

Janssen, P. A. E. M. 1989. Wave-induced stress and the drag of air flow over sea waves. *J. Phys. Oceanogr.* **19**, 745–754.

Janssen, P. A. E. M. 1991. Quasi-linear theory of wind wave generation applied to wave forecasting. *J. Phys. Oceanogr.* **22**, 1600–1604.

Janssen, P. A. E. M. 1998. On error growth in wave models. Technical Memo No 249, Research Dept, ECMWF, UK, 12 pp.

Komen, G. J., Cavaleri, L., Donelan, M., Hasselmann, K., Hasselmann, S. and Janssen, P. A. E. M. 1994. *Dynamics and Modelling of Ocean Waves.* Cambridge University Press, Cambridge, 532 pp.

Laing, A. K. and Brenstrum, E. 1996. Scatterometer observations of low-level wind jets over New Zealand coastal waters. *Wea. Forecast.*, **11**, 4, 458–475.

Lott, F. and Miller, M. 1997. A new subgrid-scale orographic parametrization: Its formulation and testing. *Q. J. R. Meteorol. Soc.* **123**, 101–127.

Miller, M., Hortal, M. and Jacob, C. 1995. A major operational forecast model change. *ECMWF News.* **70**, 2–5.

Olafsson, H. and Bougeault, P. 1996. Nonlinear flow past an elliptic mountain ridge. *J. Atmos. Sci.* **53**, 17, 2465–2489.

Pielke, R. A. 2002. *Mesoscale Meteorological Modeling.* Academic Press, New York, 676 pp.

Simmons, A. 1991. Development of the operational 31-level T213 version of the ECMWF forecast model. *ECMWF News.* **56**, 3–13.

Stull, R. B. 1988. *An Introduction to Boundary Layer Meteorology.* Kluwer, Dordrecht, 666 pp.

Teixeira, J. 1997. *The One-column Model – Reference and User's Guide.* ECMWF, Reading.

Tibaldi, S. 1986. Envelope orography and maintenance of quasi-stationary waves in the ECMWF model. *Adv. Geophys.* **29**, 339–374.

Wallace, J. M., Tibaldi, S. and Simmons, A. 1983. Reduction of systematic forecast errors in the ECMWF model through the introduction of an envelope orography. *Q. J. R. Met., Soc.* **109**, 683–717.

Zecchetto, S. and Cappa, C. 2001. The spatial structure of the Mediterranean Sea winds revealed by ERS-1 scatterometer. *Int. J. Remote Sensing* **22**, 1, 45–70.